International Journal of Nanomedicine

Dovepress
Taylor & Francis Group

Open Access Full Text Article

ORIGINAL RESEARCH

Enhanced Dermal Delivery of Nanoparticulate Formulation of *Cutibacterium acnes* Using Sponge Spicules for Atopic Dermatitis Treatment

Youmei Jin[1,2], Chi Zhang[1,2], Mengnan Jia[1,2], Ming Chen[1–5]

[1]Department of Marine Biological Science & Technology, College of Ocean & Earth Sciences, Xiamen University, Xiamen, 361102, People's Republic of China; [2]State-Province Joint Engineering Laboratory of Marine Bioproducts and Technology, Xiamen University, Xiamen, 361102, People's Republic of China; [3]Pingtan Research Institute of Xiamen University, Pingtan, 350400, People's Republic of China; [4]Shenzhen Research Institute of Xiamen University, Shenzhen, 518000, People's Republic of China; [5]State Key Laboratory of Vaccines for Infectious Diseases, Xiang'an Biomedicine Laboratory, Xiamen, 361102, People's Republic of China

Correspondence: Ming Chen, Department of Marine Biological Science & Technology, College of Ocean & Earth Sciences, Xiamen University, Xiamen, 361102, People's Republic of China, Email ming.chen@xmu.edu.cn

Introduction: The pathogenesis of atopic dermatitis (AD) is closely linked to both genetic and environmental factors, with patients often exhibiting a range of immunological abnormalities, including a pronounced Th2-type overreaction, which is a key feature of the disease.

Purpose: *Cutibacterium acnes* has been shown to induce a robust Th1 immune response through intraperitoneal injections, potentially preventing the development of AD. In this study, a novel nanoparticulate formulation of *Cutibacterium acnes* (NFCA) was developed with the formulation optimization for the dermal delivery.

Materials and Methods: Sponge *Haliclona* sp. spicules (SHS) were isolated from the explants of sponge *Haliclona sp*. with our proprietary method. The NFCA was prepared by high-speed grinding followed by film extrusion. The skin penetration of the model drugs in NFCA with SHS were visualized using confocal microscopy. The therapeutic effects of NFCA coupled with SHSs against AD in mice were assessed by using pathohistological examination and cytokine ELISA assay.

Results: The NFCA particle size was 254.1±39.4 nm, with a PDI of 0.29±0.08 and a Zeta potential of −7.9±0.6 mV. SHS significantly enhanced total skin absorption of FD10K (39.6±6.7%, p=0.00076) as well as deposition in the viable epidermis (3.2±1.6%, p=0.08) and deep skin (dermis & receptor) (36.0±5.9%, p=1.82E-5) compared to the control. In vitro cytotoxicity tests showed that NFCA had low toxicity to HaCaT cells (IC50=63.8 mg/mL). The study confirmed that NFCA can activate immune signaling pathways, promoting the high expression of IL-6 and IL-8 in keratinocytes, enhancing TNF-α and IL-1β expression in macrophages, and inducing Th1 and Th17-type immune responses. Furthermore, we demonstrated that the dermal delivery of NFCA using SHS in vivo significantly reduced epidermal thickness, serum IgE levels, and tissue IL-4 levels, thereby accelerating skin repair and mitigating Th2 polarization.

Conclusion: SHS were employed to effectively deliver NFCA to the deeper skin layers to exert its immune functions. Moreover, the combination of SHS and NFCA can significantly cure mice with atopic dermatitis.

Keywords: dermal drug delivery, sponge *Haliclona* sp. spicules, nanoparticulate formulation, *Cutibacterium acnes*, atopic dermatitis

Introduction

Atopic dermatitis (AD) is a chronic, relapsing, pruritus, noninfectious inflammatory skin disease, which is one of the common diseases in dermatology.[1] According to the Global Burden of Disease, the prevalence of AD is as high as 15–20% in children and about 10% in adults. AD also has the highest disease burden among skin diseases in terms of disability-adjusted life years.[2] This disease can lead to sleep disorders and is prone to frequent recurrence, seriously affecting the growth, development and quality of life of patients.[3,4] The exact etiology and mechanism underlying AD have not been fully understood. It is generally believed to result from a combination of factors, including genetics,[5–7] immune abnormalities,[8] impaired skin barrier function, and environmental influences,[9] with internal and external factors interacting to contribute to the disease. Currently, the primary

Received: 2 December 2024
Accepted: 6 March 2025
Published: 14 March 2025

therapeutic goals for AD are to reduce skin lesions, alleviate itching and decrease the frequency of flare-ups. Traditional topical drugs generally exert their anti-inflammatory effects through immunosuppression mechanism, but these are not suitable for long-term use. Oral medications carry the risk of nephrotoxicity and subcutaneous injections can be costly and may cause adverse reactions at the injection site. However, identifying effective drug molecules that specifically target this pathway has become a significant challenge and an area of intense research in the treatment of AD. A hallmark of AD is the tendency for CD4 lymphocytes to differentiate into Th2 lineage.[10,11] Therefore, therapeutic strategies targeting the Th2 pathway are likely to meet the needs of most patients. However, identifying effective drug molecules that specifically target this pathway has become a significant challenge and an area of intense research in the treatment of AD.

Cutibacterium acnes (formerly known as *Propionibacterium acnes*) is a Gram-positive and anaerobic rod-shaped bacterium that is symbiotic on the skin, primarily residing in sebaceous glands and hair follicles.[12,13] *C. acnes* plays both protective and pathogenic roles. It contributes to maintaining skin homeostasis by providing a protective layer on the skin and alleviating oxidative stress.[14,15] However, alterations in species or change in type of *C. acnes* may contribute to the pathogenesis of various skin diseases., A decrease in the relative abundance of *C. acnes* has been found in the lesions of patients with atopic dermatitis.[16] *C. acnes* can activate immune cells by interacting with host cell pattern recognition receptors, leading to a mixed Th1/Th17 cells response.[17–19] Consequently, some studies have attempted to reverse Th2-polarized atopic dermatitis lesions by inducing Th1 immune response through the injection of inactivated *C.acnes*, yielding significant improvements.[20]

Dermal drug delivery involves the administration of active ingredients through topical application, enabling the local therapeutic effects.[21] Compared to other routes such as traditional injection or oral administration, dermal delivery administration offers many advantages.[22,23] However, the *stratum corneum* barrier significantly limits the drug absorption through the skin. To address this challenge, various enhancement techniques have been developed, including, chemical permeation enhancers,[24] iontophoresis,[25] sonophoresis,[26] electroporation,[27] NFCArriers,[28] microneedles[29] and among others. Sponge *Haliclona* sp. spicules (SHS) is a type of dispersed silicon microneedles, characterized by a uniform size and shape (about 120 μm in length and 7 μm in diameter). SHS can form numerous nanoscale microchannels on the skin surface through[30–34] a minimally invasive physical process, facilitating the dermal absorption of various therapeutics without the risk of bleeding or infection. Moreover, it is not constrained by the application area or site.

In this study, we developed and characterized a nanoparticulate formulation of *Cutibacterium acnes* (NFCA). We then investigated the immune response of skin cells to NFCA by assessing the mRNA expression levels of IL-6, IL-8, TNF-α, and IL-1β. Additionally, we utilized SHS to topically deliver NFCA as an antigenic agent for the treatment of atopic dermatitis in both in vitro and in vivo.

Materials and Methods

Chemicals and Animals

The *C. acnes* strain was obtained from the Guangdong Microbial Culture Collection Center (Guangzhou, China). Soybean Phospholipid was purchased from Tianfeng Pharmaceutical Co., Ltd (ShenYang, China). Fluorescein isothiocyanate-dextrans 10K were purchased from Sigma (St. Louis, MO, USA). RAW264.7 cell and HaCaT cell were purchased from FuHeng Biotechnology Co., Ltd (ShenYang, China). And all other chemicals used in this study were of analytical grade and were purchased from Sinopharm Group Co. Ltd. (Shanghai, China).

The porcine skin was obtained from YinXiang Group Co., Ltd. (Xiamen, China). BALB/c mice and Guinea pigs were purchased from Vital River Laboratory Animal Technology Co., Ltd. (Beijing, China). Animal experiments were carried out in compliance with the "Regulations on the Administration of Laboratory Animals of Xiamen University" and received approval from the Institutional Animal Care and Use Committee of Xiamen University (Ethics Approval No. XMULAC20240005).

Preparation of NFCA

400 mg soybean phospholipid, 100 mg Tween 80, 2 g propylene glycol, and 10 mg freeze-dried Cutibacterium acnes were diluted to 10 g with deionized water. 1 g of this suspension and 30 ceramic beads (3 mm diameter) were added to a sterile 5 mL grinding tube. Nanoparticulate formulation of *Cutibacterium acnes* (NFCA) was prepared using a cryogenic grinder

(MB-48LD-1, MeiBi Co. Ltd., Shanghai, China) at −40°C, oscillating at 70 hz for 120 s, pausing for 10s, and repeating for 12 cycles (250 s per cycle). NFCA was stored at 4°C for further use. The extruded NFCA (eNFCA) was prepared using our previous method[31] by extrusion through a 100 nm polycarbonate membrane (AVESTIN, Inc., Ottawa, ON, Canada) using a liposome extruder (LiposoFast, AVESTIN, Inc., Ottawa, ON, Canada) for 21 times.

Characterization of NFCA

The size distribution and ζ-potential of NFCA were measured using a photon correlation spectroscopy (Zetasizer Nano series, Malvern Instruments Ltd, Worcestershire, UK) NFCA were diluted 100 times with deionized water before the measurement. Cryo-transmission electron microscopy (FEI Tecnai F20S, Hillsboro, OR, USA) was utilized to observe the morphology of NFCA and eNFCA. Each sample was diluted 10 times and fixed on the copper mesh adapted to the TEM. After cooling with liquid nitrogen, the sample rod equipped with the copper mesh should be inserted into the sample table of the transmission electron microscope, waiting for the end of vacuuming, and then observed under the condition of 80.0kV. To measure the total protein in NFCA or eNFCA, 1% Triton X-100 solution was weighed with phospholipid at 10:1 ratio, mixed with oscillator, and incubated at room temperature for 30 min. The absorbance value was measured at 562 nm wavelength using an enzymoscope, and the amount of total protein was calculated according to the standard curve.

Skin Penetration Study in vitro

The isolated porcine back skin was used and thawed at room temperature before the in vitro experiment. The circular skin sections were punched out and positioned on the Franz diffusion cell (the effective penetration area of 1.77 cm^2) with the stratum corneum (SC) side facing up. The receptor chamber was pre-filled with 0.2 M PBS solution, and skin conductance was measured (<5μA) to ensure the integrity of the skin barrier. SHS (100 μL, 100 mg/mL in PBS) was topically applied on the skin surface with a massage duration of 120 seconds (300 r/min). The test formulations containing 300 μL hydrophilic (FD10K) or 200 μL lipophilic (DiD) model drugs were designed as following:

1) FD10K control group (FD10K in water, 1 mg/mL), 2) FD10K@NFCA group (FD10K in NFCA solution, 1 mg/mL), 3) SHS + FD10K@NFCA group (FD10K in NFCA solution, 1 mg/mL), 4) DiD control group (DiD in 10% DMSO solution, 0.02 mg/mL), 5) DiD@NFCA group (DiD in NFCA solution, 0.02 mg/mL) and 6) SHS + DiD@NFCA group (DiD in NFCA solution, 0.02 mg/mL). The test formulations were evenly distributed on the donor compartment of Franz diffusion cell. The temperature of the water bath was 37°C, and the stirring speed was 600 rpm. Each cell was placed into the water bath, ensuring the receptor chamber was submerged. A small magnetic stir bar was added to the receptor chamber. The system was kept away from light during the experiment. After 16 hours, the remaining test formulations in the donor compartment was washed with PBS five times until no visible residue remained. The porcine skin was carefully removed, placed on aluminum foil, dried, and labeled for further analysis. Additionally, 1 mL of the receptor solution was collected and stored at 4°C, protected from light for future analysis. The SC layers were obtained by using the tape-stripping method.[30,31] The glass bottles containing each layer were collected, 4 mL of extract solution (methanol and 0.05M PBS, 1:1, V/V) was added, and then extracted in a shaking table at 26°C and 180 rpm for 24 h. After extraction, each tube was centrifuged at 5000 rpm for 5 min and left for testing. The skin deposition of FD10K in different skin layers were measured at the excitation wavelength of 490 nm and the emission wavelength of 530 nm.

The skin penetration of the model drugs in NFCA were also visualized using confocal microscopy (Carl Zeiss, LSM780NLO, Jena, Germany). After the in vitro skin penetration experiment, a small skin sample with a radius of 2.5 mm was punched out and quickly preserved in OCT compound. The porcine skin was then sectioned into 10 μm slices. The prepared sample was then examined using a confocal microscope.

Cytotoxicity and Immune Response of Skin Cells to NFCA in vitro

Cytotoxicity of NFCA was assessed using the MTT assay. Logarithmic-phase HaCaT cells were collected, and the cell suspension concentration was adjusted to 5×10^4 cells/mL. A total of 200 μL of the cell suspension was added to each well of a 96-well plate and incubated for 24 hours. NFCA solutions were prepared at different concentrations: 100 mg/mL, 50 mg/mL, 25 mg/mL, 10 mg/mL, 5 mg/mL, 1 mg/mL, 0.5 mg/mL, and 0.1 mg/mL. The blank control group did not add any NFCA. The NFCA solutions were incubated with the cells for 24 hours. After incubation, MTT solution was added and cultured for another 4 hours, followed by the addition of 10 μL of Formazan solution. The plate was placed on a shaker for 10 minutes at low speed

to fully dissolve the purple crystals. Absorbance was measured at 490 nm using a microplate reader. Similarly, HaCaT cells were incubated with NFCA solutions at varying concentrations for 24 hours. Total RNA was extracted using a column animal tissue RNA extraction and purification kit (ShengGong Co. Ltd., Shanghai, China). RNA concentration was measured, reverse-transcribed into cDNA, and target fragments were amplified via PCR to obtain electrophoresis bands for IL-6 and IL-8.
The sequence of primers used is as follows:
IL-8-F: CTGATTTCTGCAGCTCTGTG
IL-8-R: GGGTGGAAAGGTTTGGAGTATG
IL-6-F: AGCCACTCACCTCTTCAGAAC
IL-6-R: GCCTCTTTGCTGCTTTCACAC
GAPDH-F: GCAGTGGCAAAGTGGAGATT
GAPDH-R: CGCTCCTGGAAGATGGTGAT
After that, cytotoxicity test and cell co-culture stimulation experiment were performed on RAW264.7 cells according to the same procedure above.
The sequence of primers used is as follows:
TNF-α-F: AAAAGCAAGCAGCCAACCAG
TNF-α-R: GCCACAAGCAGGAATGAGAA
IL - 1β- F: TGAAGGGCTGCTTCCAAACCTTTGACC
IL - 1-β-R: TGTCCATTGAGGTGGAGAGCTTTCAGC
β-actin - F: TGGAATCCTGTGGCATCCATGAAAC
β-actin - R: TAAAACGCAGCTCAGTAACAGTCCG

Mice Modeling of Atopic Dermatitis

1 mg of MC903 (molecular weight 412.60) was dissolved in 2.424 mL of anhydrous ethanol to prepare a 1 mm solution. This was further diluted 10-fold to obtain a 0.1 mm MC903 working solution, which was aliquoted into 1.5 mL centrifuge tubes (1 mL per tube) and stored at −20°C. BALB/c female mice, aged 8–10 weeks, were randomly divided into three groups: a negative control group, an ear modeling group treated with MC903 for 7 days, and another ear modeling group treated with MC903 for 14 days, with three mice in each group. All mice were housed individually in the Laboratory Animal Center of Xiamen University.

The experiment lasted 14 days, with daily application of the solution. In the normal control group, the left ear was treated with anhydrous ethanol, while the modeling groups received 20 μL of MC903 working solution on the back of the left ear. Photographs were taken on days 0, 7, and 14, and transepidermal water loss (TEWL) values were measured using a TEWL meter (Courage Khazaka electronic GmbH, Koeln, Germany).

Samples were collected on days 7 and 14. Mice were euthanized via cervical dislocation, and the ears were excised at the base. Circular skin sections of uniform diameter were punched from the ears. After embedding, pathological sections were prepared, and H&E staining was used to observe inflammatory cell infiltration in the skin. Additionally, ear tissue homogenate supernatant was prepared, and Thymic Stromal Lymphopoietin (TSLP) levels in the ear tissue were measured using an ELISA kit (Solarbio Science & Technology Co.,Ltd. Beijing China).

Treatment of Atopic Dermatitis in Mice

BALB/c mice, aged 8–10 weeks, were randomly assigned into six groups with three mice per group: a negative control group, a 7-day modeling group, a self-healing group, a low dosage NFCA treatment group, a medium dosage NFCA treatment group, and a high dosage NFCA treatment group. All mice were housed individually in separate cages at the Laboratory Animal Center of Xiamen University. During the first 7 days of the 14-day experiment, all groups, except the negative control group, underwent modeling. A 20 μL MC903 working solution was applied to the dorsal side of the left ear of the mice. On the 8th day, the 7-day modeling group was sampled. Starting from day 8, the self-healing group received no further treatment, while the treatment groups were rubbed manually for 2 minutes daily with a 20 μL SHS suspension (SHS = 2 mg). To minimize stress, the mice were temporarily anesthetized using an anesthesia machine before the massage. After the massage, different doses of Nano.acnes solution were applied to the ears: 0.1 mg/cm^2 of

NFCA for the low dosage treatment group, 0.2 mg/cm^2 for the medium dosage group, and 0.4 mg/cm^2 for the high dosage group. The treatment phase lasted from day 8 to day 14, for a total of 7 days. After the experiment, blood of each mouse was collected via orbital puncture, and serum IgE levels were measured. Ear tissue homogenates were prepared to assess IL-4 levels. Frozen sections were made from each group, and the epidermal thickness was measured under a microscope at 200× magnification.

Skin Toxicity of NFCA in Guinea Pig

After anesthetizing guinea pigs with ether, the hair on their backs was carefully shaved. Experimental points were marked on their backs, grouped and numbered as required, with a 2×2 cm square area designated for each point. The experiment was divided into two groups and each group was stimulated once daily for 7 days. No treatment for the control group. For the NFCA in combination with SHS group: A 60 μL SHS aqueous solution (SHS = 6 mg) was applied to the skin of the designated area for 2 minutes, followed by 0.6 g of Nano.acnes solution containing 0.6 mg of NFCA. After the experiment, skin tissue was collected to prepare sections for histological staining and observation. Skin irritation induced by NFCA combined with SHS was assessed using skin irritation response scores and skin irritation intensity evaluation criteria according to published research.[35]

Data Analysis

All experiments in this study were performed in triplicate at least. All data were expressed as the mean value ± S.D. Two-tailed and unpaired Student's t test were performed and $p < 0.05$ is considered to be significant. All image data was analyzed by Image J software.

Results and Discussion

Preparation and Characterization of NFCA

For effective dermal delivery, it is necessary to reduce the size of *Cutibacterium acnes* to the nanoscale. We achieved this by incorporating phospholipids into the *Cutibacterium acnes* suspension containing 20% (W/W) propylene glycol, then nanoparticulating the entire system into a nanoparticulate formulation (NFCA) using a cryogenic grinder. Tween 80 was also incorporated into the system due to its single-tail chemical structure, which enables rapid adsorption at interfaces, thereby assisting in further particle size reduction.[36] The phospholipids and Tween 80 helped reduce the aggregation of bacterial lysate over time at 4°C (Figure 1a). We also optimized the grinding cycles and the ratio of phospholipids to Tween 80 in terms of particle size distribution and polydispersity index (PDI) of the NFCA (Figure 1b–d). Additionally, we extruded NFCA through a 100 nm polycarbonate membrane (AVESTIN, Inc., Ottawa, ON, Canada) to further decrease the particle size to obtain extruded NFCA (eNFCA). However, this process led to significant total protein loss (Figure 1e). The NFCA and eNFCA were characterized by using TEM and photon correlation spectroscopy. The NFCA displayed inhomogeneous solid vesicles with several antenna-like projections (Figure 1f) with a mean diameter of 254.2 ±39.4 nm, a PDI of 0.29 ±0.08, and a ζ-potential of −7.9±0.6 mV. The eNFCA display a smaller particle size with a mean diameter of 132.30±0.08 nm and a PDI of 0.22±0.59 (Figure 1g).

The Immune Response of Different Skin Cells to NFCA

Keratinocytes are the first skin cells exposed to NFCA. To evaluate the toxicity of NFCA on HaCaT cells, the cell viability was measured using thiazole blue colorimetry (MTT) (Figure 2a). The half-maximal inhibitory concentration (IC50) was calculated for both NFCA (63.8 mg/mL) and eNFCA (15.2 mg/mL). Compared to NFCA, eNFCA was more cytotoxic at lower concentrations. We speculate that the therapeutic protein is unable to pass through the membrane and may be lost during the extrusion process. In contrast, toxic components can extruded through the membrane and become enriched. Consequently, eNFCA exhibits a lower protein content but significantly higher cytotoxicity in HaCaT cells.

Heat-inactivated *Cutibacterium acnes* has been shown to significantly up-regulate the expression of IL-6 and IL-8 in HaCaT cells in a dose-dependent manner.[37] IL-6 and IL-8 are involved in neutrophil recruitment. By detecting these two cytokines, we can assess whether NFCA retains antigenic properties similar to intact bacteria. Based on the calculated

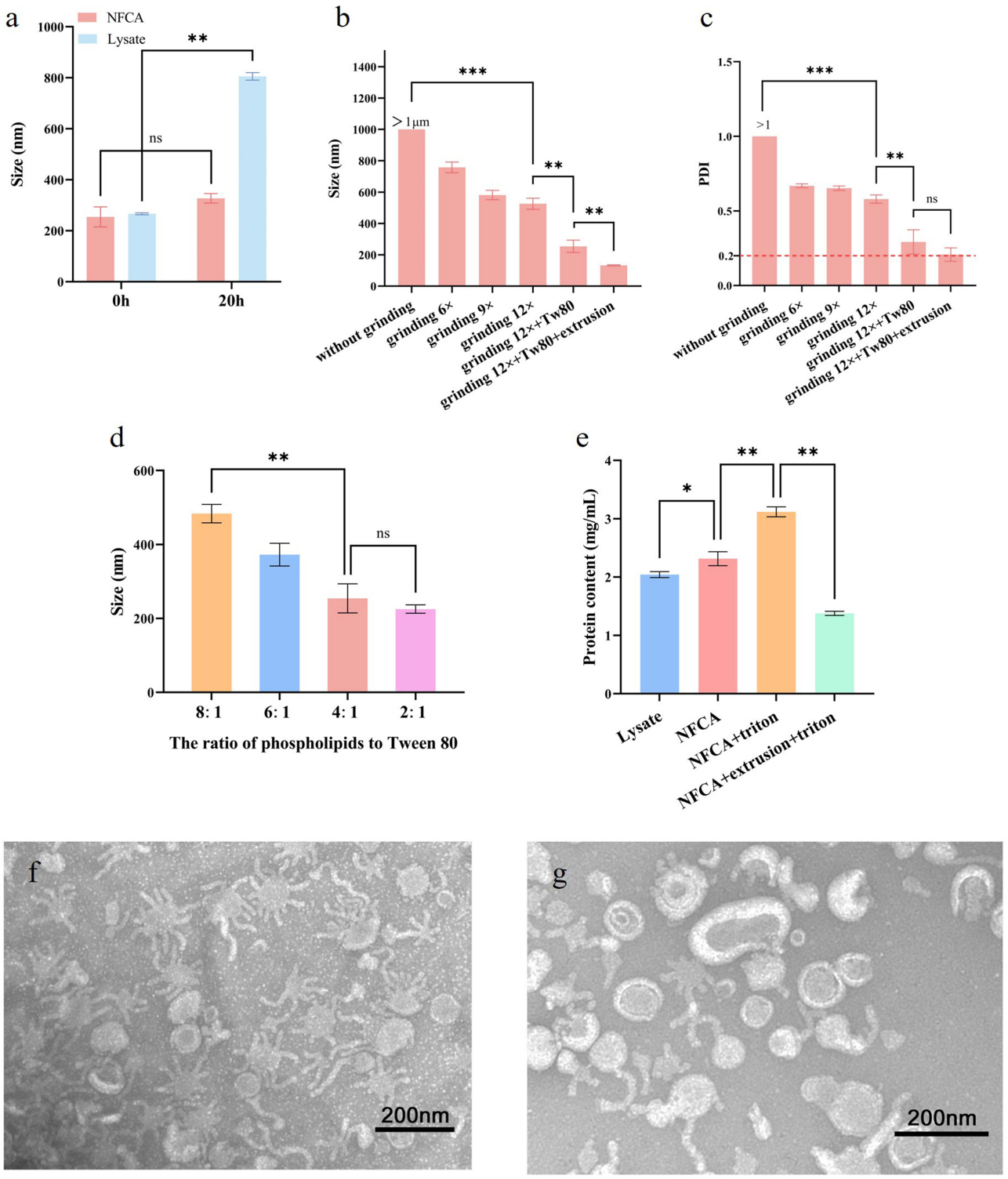

Figure 1 The preparation and characterization of NFCA. (**a**) Size changes of the bacterial lysate and NFCA before and after 20 hours of preparation. (**b**) The effect of grinding cycle numbers, Tween 80 addition, and extrusion on particle size. (**c**) The impact of different grinding cycle numbers, Tween 80 addition, and extrusion on PDI. (**d**) The influence of the phospholipid-to-Tween 80 ratio on particle size. (**e**) Comparison of protein content across systems. (**f**) TEM image of NFCA. (**g**) TEM image of eNFCA. *Statistically was different from other groups ($p < 0.05$). ** Statistically very different from other groups ($p < 0.01$). *** Statistically extremely different from other groups ($p < 0.001$).

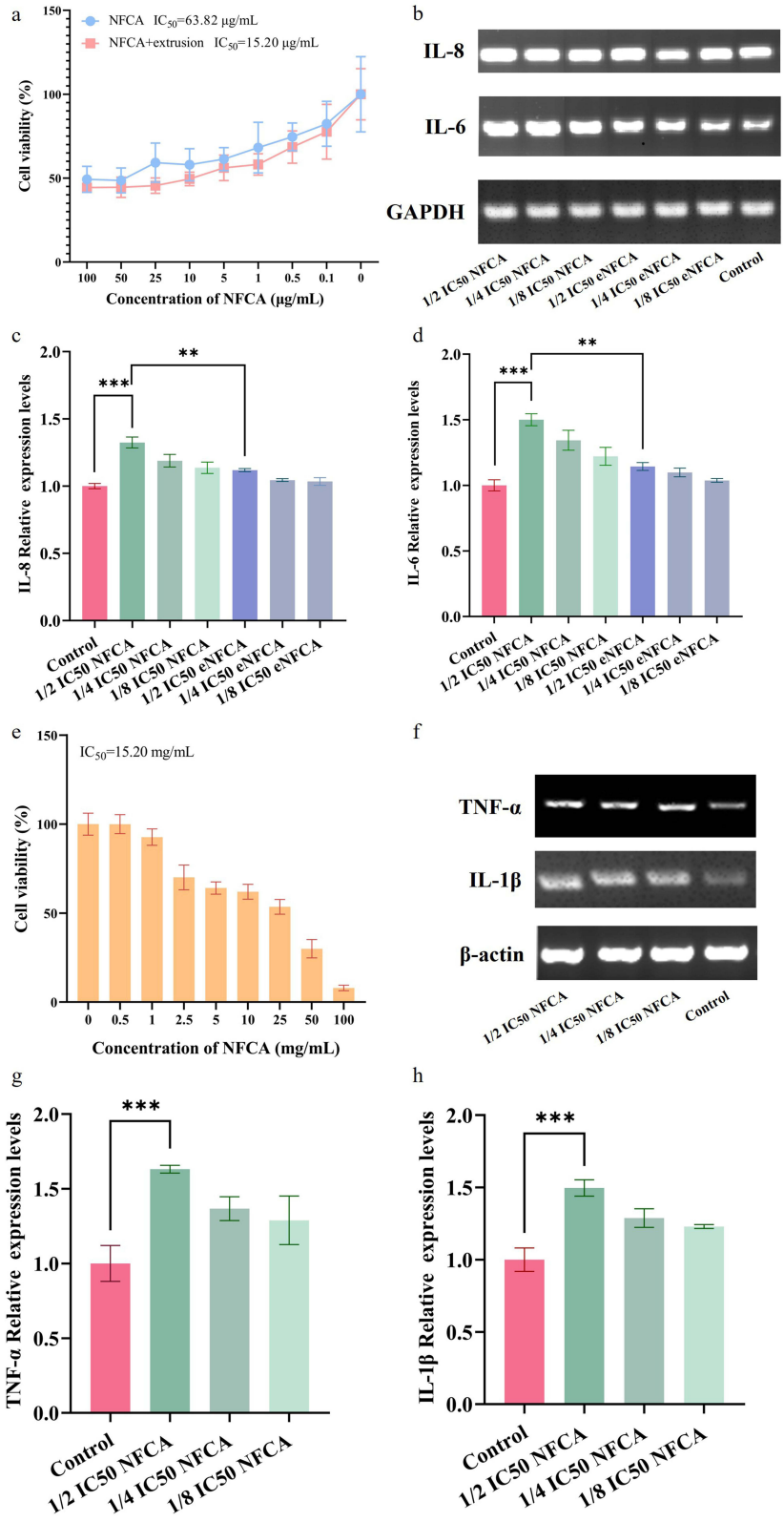

Figure 2 The immune response of different skin cells to NFCA. (**a**) Survival rate (%) of HaCaT cells at different concentrations of NFCA and eNFCA. (**b**) Electrophoretic analysis of GAPDH, IL-6, and IL-8 proteins. (**c**) Comparison of IL-8 mRNA expression levels. (**d**) Comparison of IL-6 mRNA expression levels. (**e**) Survival rate (%) of RAW264.7 cells at different concentrations of NFCA. (**f**) Electrophoretic analysis of β-actin, TNF-α, and IL-1β proteins. (**g**) Comparison of TNF-α mRNA expression levels. (**h**) Comparison of IL-1β mRNA expression levels. ** Statistically very different from other groups ($p < 0.01$). *** Statistically extremely different from other groups ($p < 0.001$).

https://doi.org/10.2147/IJN.S509798

IC50, we established three concentration gradients (1/2 IC50, 1/4 IC50, 1/8 IC50) for both groups (Figure 2b). After 24 hours exposure, the total RNA was extracted from the cells and reverse-transcribed into cDNA. RT-PCR was used to detect differences in IL-6 and IL-8 mRNA expression. We found that NFCA can significantly up-regulate the expression of IL-6 (Figure 2c) and IL-8 (Figure 2d) in HaCaT cells in a dose-dependent manner.

Macrophages, key players in the skin's immune system, help ones understand the specific immune responses induced by NFCA, which is crucial for its mechanism in treating atopic dermatitis. Macrophages constantly monitor the skin microenvironment for signs of cellular stress, tissue damage, or infection.[38] In response to infection, they initiate adaptive inflammation aimed at restoring homeostasis.[39,40] Atopic diseases often exhibit Th2-type polarization, but key Th1-type cytokines can trigger Th1 immune responses, preventing or even reversing Th2-dominant phenomena.[41] TNF-α is a pleiotropic cytokine and a key player in the Th1 signaling pathway,[42] while IL-1β activates innate immune cells, including antigen-presenting cells, driving CD4+ T cell differentiation into Th17 cells.[43]

We then co-cultured NFCA with RAW264.7 cells for 24 hours to evaluate its cytotoxicity (Figure 2e). Next, we measured the expression of TNF-α and IL-1β induced by NFCA across different IC50 concentration gradients (Figure 2f). The results showed that NFCA directly stimulated a dose-dependent increase in TNF-α (Figure 2g) and IL-1β (Figure 2h) expression in RAW264.7 cells.

The Dermal Delivery of NFCA Using SHS in vitro

Based on the characterization and cytotoxicity results of NFCA and eNFCA, we selected NFCA for further investigation. The exact active components of NFCA responsible for atopic dermatitis (AD) treatment are not yet fully understood. To evaluate the skin penetration and deposition behavior of NFCA, we utilized FD10K, a fluorescent glucan with a large molecular weight, as a model drug for the hydrophilic components, and DiD, a fluorescent dye, as a model drug for the lipophilic components in NFCA. While the total skin absorption (2.4±0.6%) and deposition in the viable epidermis (0.5 ±0.2%) and deep skin (dermis and receptor) (1.1±0.4%) for both model drugs in NFCA were slightly lower than those in the solvent system (control group), these differences were not statistically significant (p>0.5). However, SHS significantly enhanced total skin absorption (39.6±6.7%, p=0.00076) as well as deposition in the viable epidermis (3.2±1.6%, p=0.08) and deep skin (dermis and receptor) (36.0±5.9%, p=1.82E-5) compared to the control (Figure 3a). We also visualized the skin penetration and distribution of the two model drugs, with and without SHS (Figure 3b and c). These findings indicated that SHS can effectively enhance the delivery of NFCA's active components into deeper skin layers.

The Dermal Delivery of NFCA Using SHS for AD Treatment in Mice

MC903 stimulates the high expression of TSLP via the vitamin D receptor in keratinocytes. TSLP mediates the Th2 allergic inflammatory response, promoting the elevated expression of Th2 cytokines such as IL-4 and IL-13 in Th2 cells, thereby inducing AD-like inflammation in both the skin and the body.[44] Ear swelling, keratinization, hyperkeratosis, irregular thickening of the spinous layer, and infiltration of inflammatory cells in the dermis were observed in all mice in the modeling group (Figure 4a). Additionally, TEWL values and tissue TSLP levels were significantly increased (Figure 4b and c). We selected two time points for evaluation: one after 7 days of continuous stimulation and the other after 14 days. After 14 days, ear dryness in the mice worsened, and the skin damage became uneven. At this stage, topical application of SHS could further harm the skin, potentially hindering the AD treatment. Considering that TEWL levels and TSLP expression were significantly elevated by day 7, we concluded that the AD model was successfully established on day 7 and we launched the AD treatment using NFCA in combination with SHS at day 8.

We investigated the effectiveness of NFCA at different dosage for AD treatment in MC903 mice model. While there was no significant difference among these groups in overall appearance, histopathological sections revealed that after a period of self-healing or NFCA treatment, the thickness of the epidermal layer was reduced to varying degrees (Figure 5a and b). Before the treatment, the epidermal layer of MC903 mice were dramatically thickened to 70.6±7.7 μm. In the self-healing group, the epidermal thickness decreased to 49.5±7.7 μm after 7 days. In the NFCA treatment groups, epidermal thickness was reduced to 40.5±1.8 μm with low dosage NFCA (0.1 mg/cm^2), to 29.4±4.1 μm with medium dosage NFCA (0.2 mg/cm^2), and to 42.3±17.6 μm with high dosage NFCA treatment (0.4 mg/cm^2) (Figure 5b).

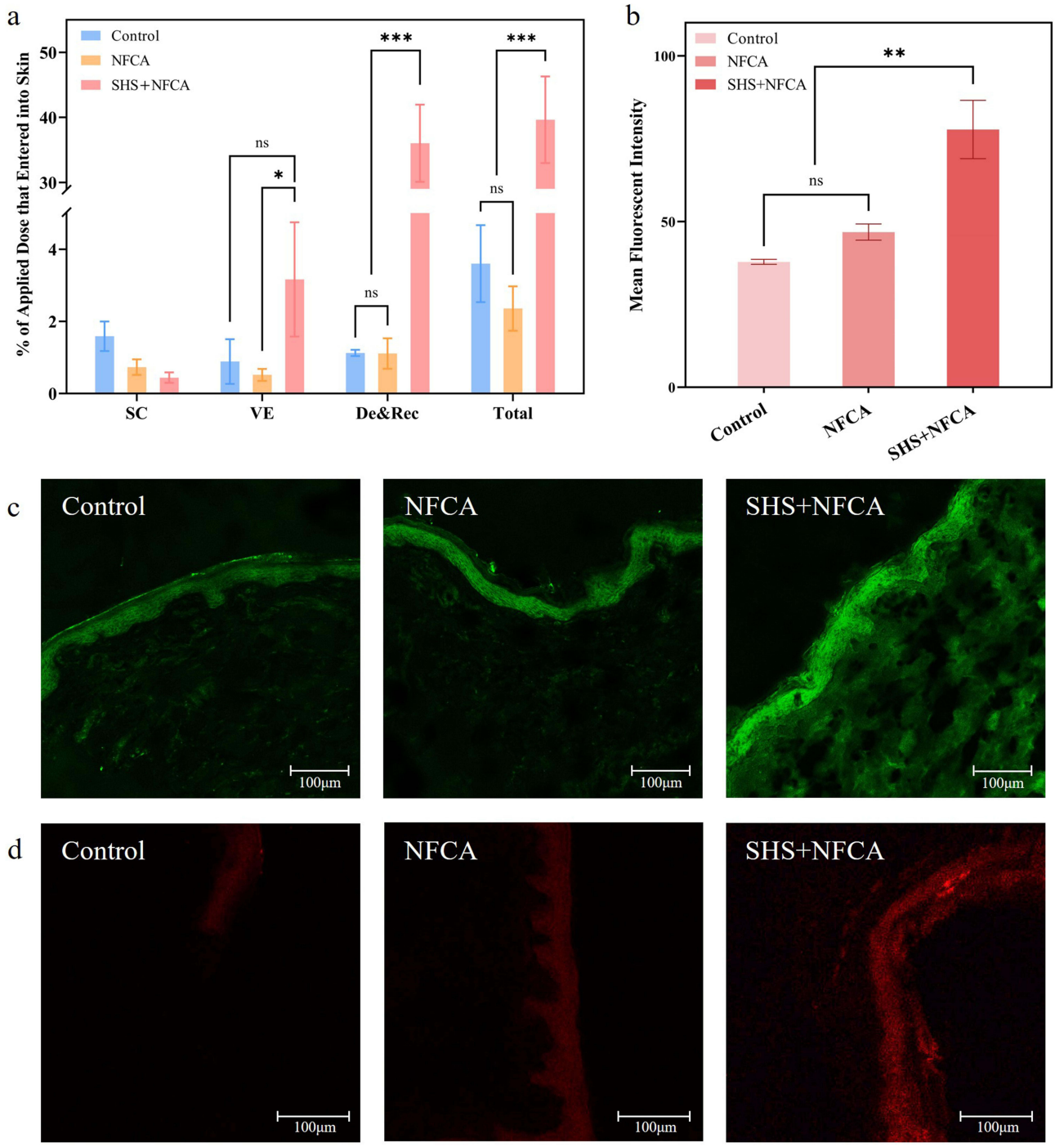

Figure 3 The dermal delivery of NFCA in vitro. (**a**) Skin penetration and deposition of FD10K as a hydrophilic model drug in NFCA with or without using SHS. (**b**) Skin absorption of DiD as a hydrophobic model drug in NFCA with or without using SHS. (**c**) Confocal visualization of FD10K skin penetration with or without using SHS. (**d**) Confocal image of DiD skin penetration with or without using SHS. * Statistically was different from other groups ($p < 0.05$). ** Statistically very different from other groups ($p < 0.01$). *** Statistically extremely different from other groups ($p < 0.001$).

Elevated IgE levels are a hallmark of AD, promoting the degranulation of mast cells and basophils, which in turn amplifies the Th2 immune response. Th2 cytokine IL-4 provides activation signals for B cells, further enhancing autoreactive IgE synthesis and release.[45,46] Serum IgE levels in the mice followed a similar pattern to the changes in epidermal thickness, with the lowest IgE levels observed in the medium dosage NFCA group (5013.2±2077.2 pg/mL)

https://doi.org/10.2147/IJN.S509798

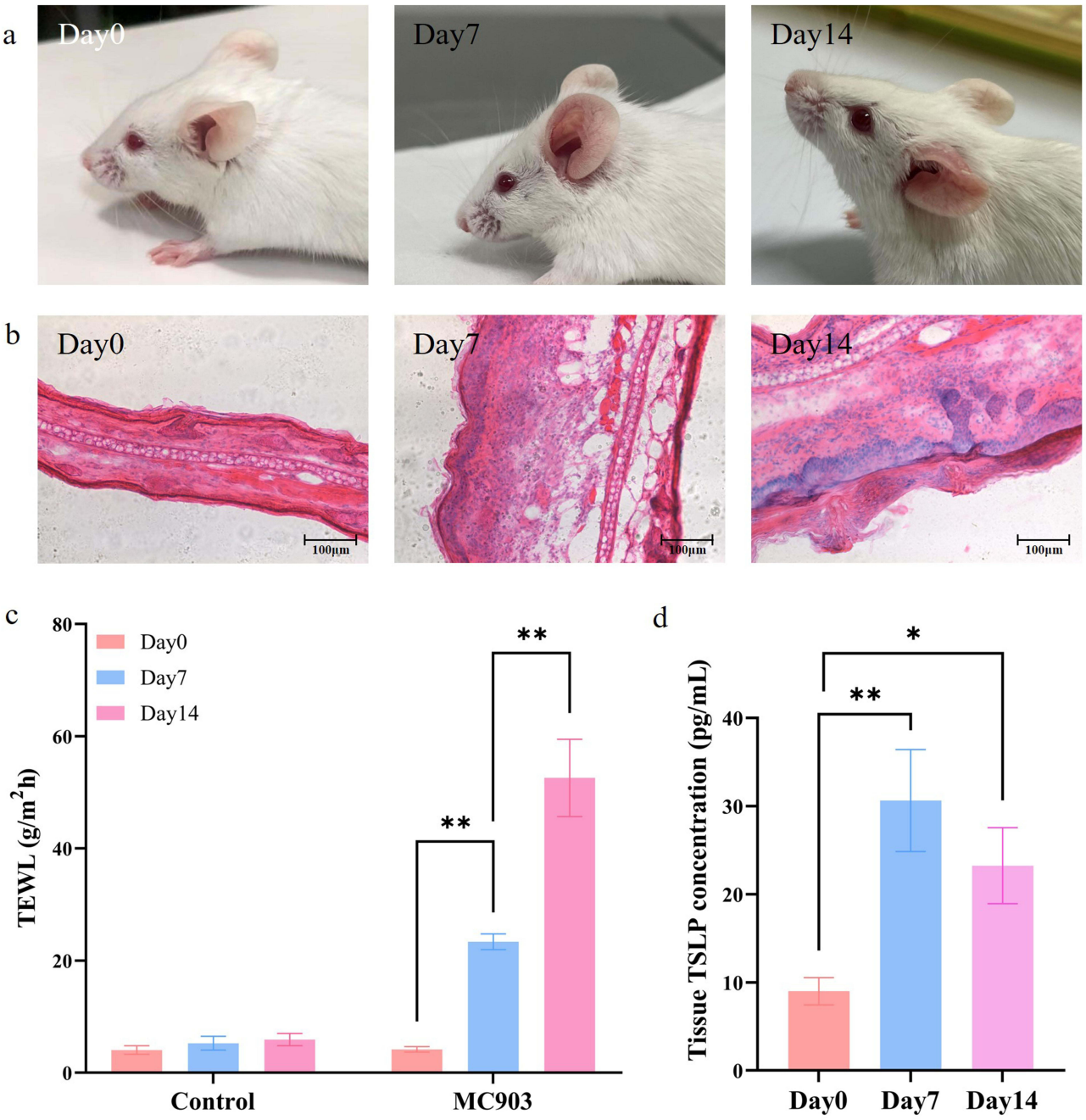

Figure 4 Mouse model of atopic dermatitis. (**a**) Appearance of AD mice induced by MC903. (**b**) Pathological section of AD mice induced by MC903. (**c**) Comparison of TEWL levels in AD mice induced by MC903. (**d**) Comparison of tissue TSLP levels in AD mice induced by MC903. * Statistically was different from other groups ($p < 0.05$). **Statistically very different from other groups ($p < 0.01$).

(Figure 5c). However, high dosage NFCA promoted elevated IgE levels, suggesting a possible overactive immune response, potentially due to immune effects from certain components in NFCA.

IL-4 levels in skin tissue decreased as NFCA dosage increased, with the medium dosage NFCA (539.8±41.2 pg/mL) and high dosage NFCA (508.4±16.9 pg/mL) groups showing significantly lower IL-4 levels than the self-healing group (Figure 5d), indicating successful suppression of the Th2 response. This result aligned with the findings reported by Hiroshi Kitagawa et al.[20] However, compared to injection, the combination of SHS and NFCA was potentially a safer and more convenient method.

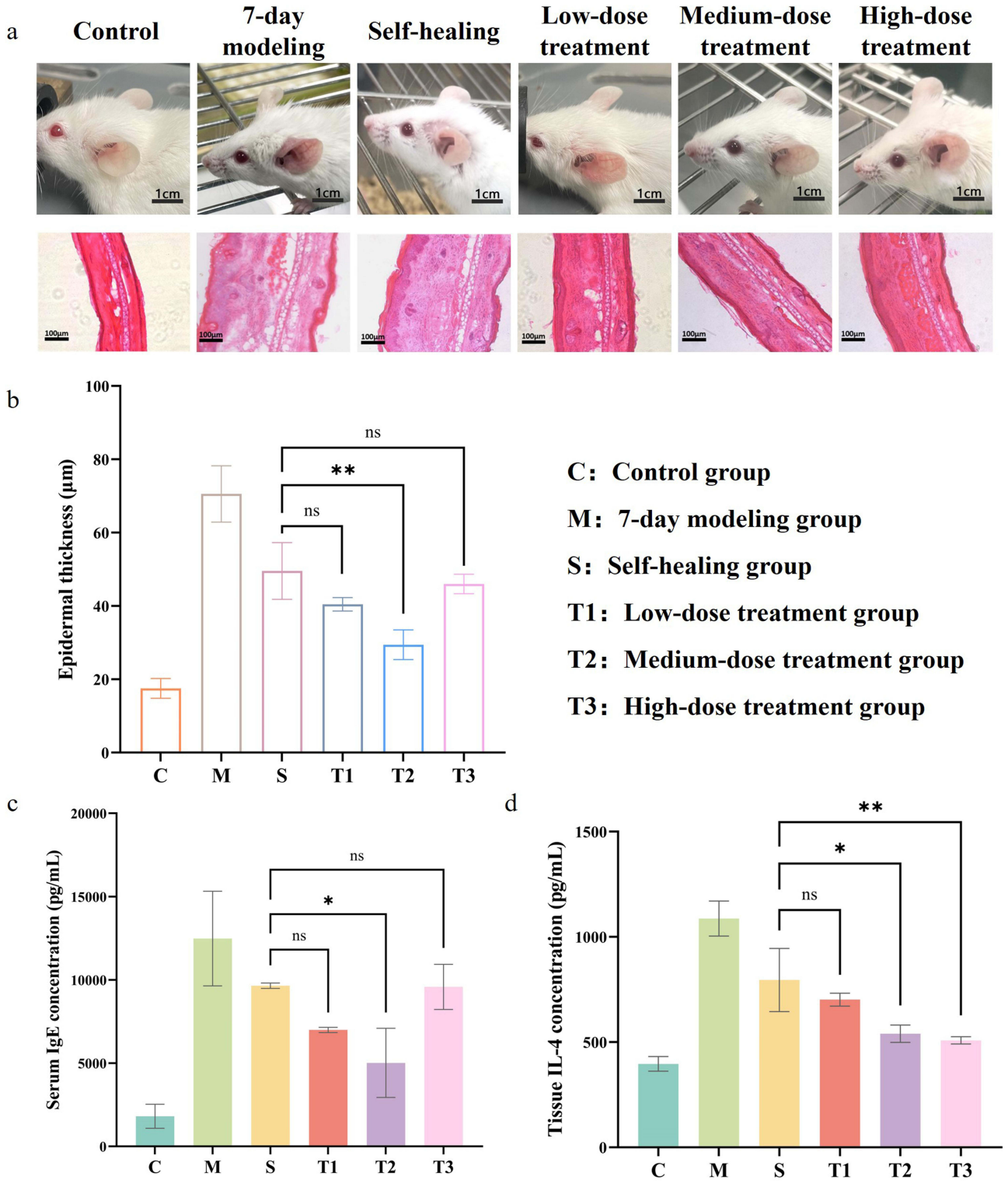

Figure 5 The AD treatment in mice using NFCA in combination with SHS. (**a**) Appearance and pathological sections of each group of mice in the treatment experiment. (**b**) Statistical comparison of epidermal thickness. (**c**) Comparison of serum IgE levels. (**d**) Comparison of tissue IL-4 levels. * Statistically was different from other groups ($p < 0.05$). **Statistically very different from other groups ($p < 0.01$).

https://doi.org/10.2147/IJN.S509798

Based on above results in vivo, we speculated the potential mechanism of action of the topical application of NFCA in combination with SHS for AD treatment as following (Scheme 1):

1. SHS create a large number of nanoscale-channels in SC to enhance the dermal delivery of NFCA which contains antigens responsible for AD treatment. Keratinocytes (KCs), the first cells to come into contact with these antigens, highly express cytokines such as IL-6 and IL-8, initiating the skin immune response and recruiting related immune cells. IL-6 can induce B cell proliferation, differentiation, and antibody production, potentially facilitating the Ig category switch.
2. Macrophages (Mø) recognize signals transmitted by keratinocytes or directly identify the antigens involved in NFCA, secreting cytokines like TNF-α and IL-1β. Dendritic cells in the epidermis, specifically Langerhans cells (LCs), capture the antigens and migrate to the dermis under the influence of cytokines such as IL-1β and TNF-α. These cells produce cytokines like IL-12 and, guided by chemokines, present the antigens to T cells in the lymphoid tissue.
3. Antigen-sensitized CD4+ Th cells (Th0) differentiate into Th1 cells, which secrete cytokines such as IFN-γ and IL-12. This process inhibits the secretion and proliferation of Th2 cells, leading to a decrease in Th2 cytokines like IL-4. Consequently, IL-4-induced IgE levels are reduced.

Consequently, the Th1/Th2 imbalance is improved, and type I hypersensitivity is diminished.

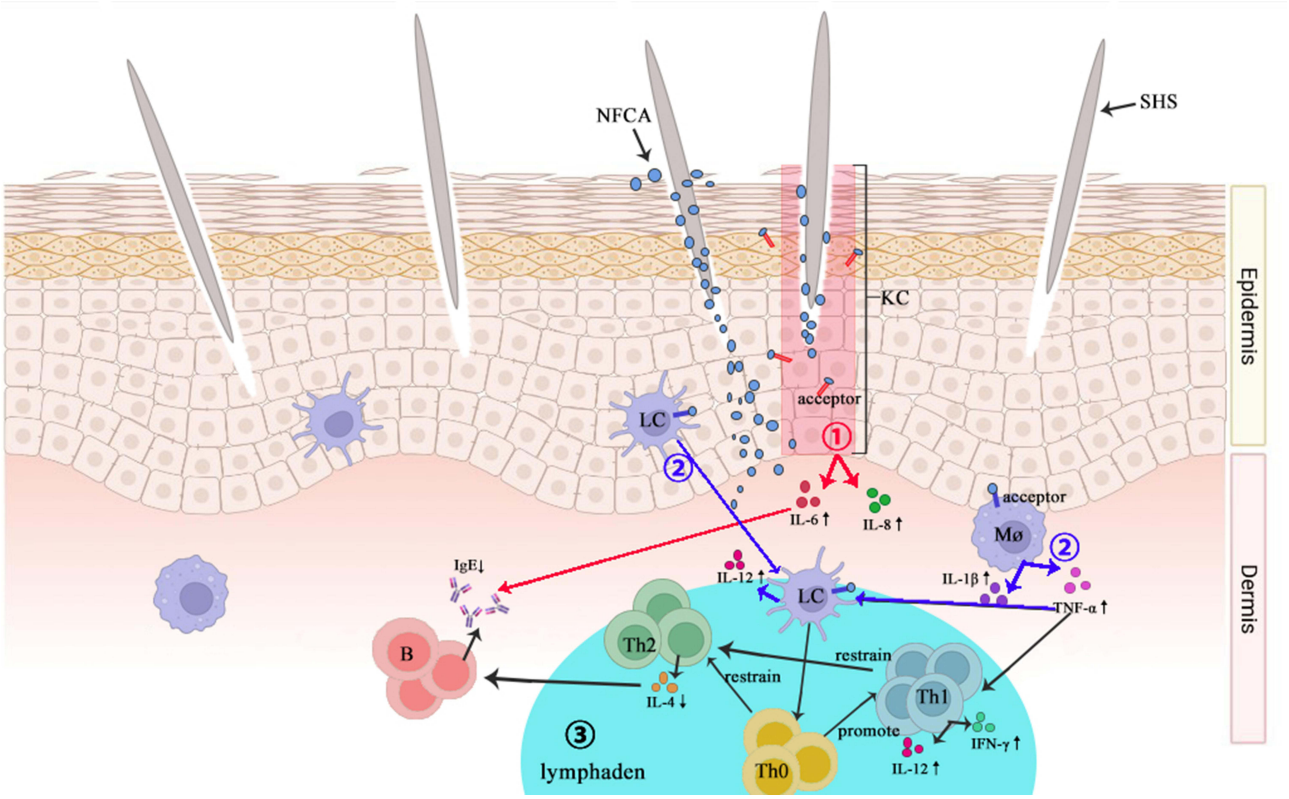

Scheme 1 The potential mechanism of action of the topical application of NFCA in combination with SHS for AD treatment. The process ① represents the keratinocyte recognition and its immune response (red arrow); The process ② involves the recognition and immune response of active immune cells (including Langerhans cells and macrophages) in the skin (blue arrow); The process ③ depicts the immune response after NFCA presented to the lymph nodes (black arrow).
Abbreviations: KC, keratinocyte; LC, Langerhans cells; Mø stands, macrophage; B, B cell; Th0 represents CD4+Th cells that have been sensitized by the antigen; Th1, type 1 helper T lymphocyte; Th2, type 2 helper T lymphocyte.

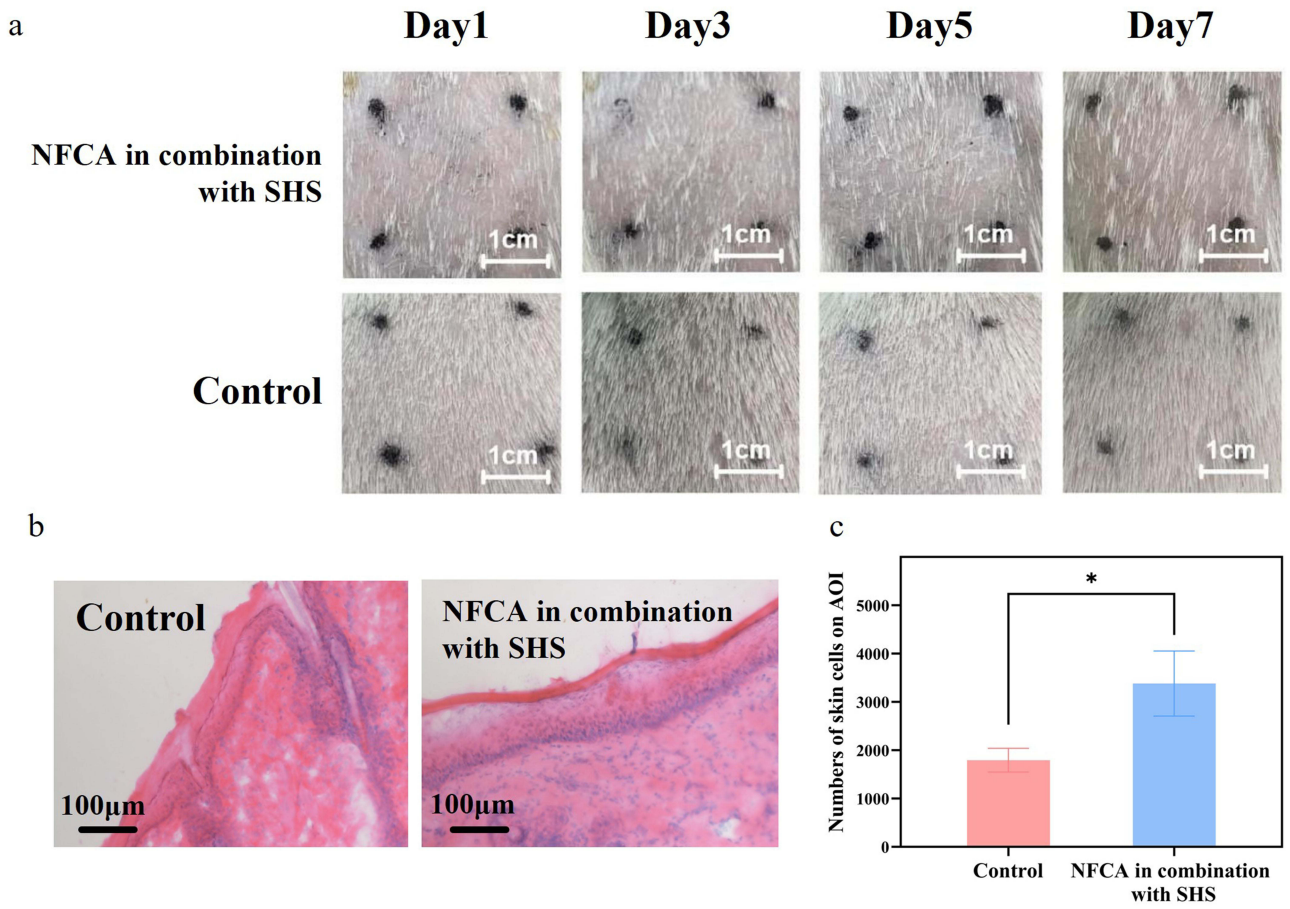

Figure 6 Skin Toxicity of NFCA in combination with SHS. (**a**) In vivo skin irritation study on Guinea pig skin using NFCA in combination with SHS. (**b**) H&E stained sections of the control group and NFCA in combination with SHS. (**c**) Statistical comparison of skin cell count in the area of interest (AOI). * Statistically was different from other groups ($p < 0.05$).

Skin Toxicity of NFCA in Combination with SHS in vivo

We next investigated the skin toxicity of the topical application of NFCA in combination with SHS over time in guinea pigs. There was no significant abnormalities over the whole treatment period. The skin showed no signs of swelling or erythema, though there was slight desquamation (Figure 6a). Based on the skin irritation scoring criteria, the scores over the 7-day period were 0, 0, 0, 0, 0.5, and 0.5, indicating that NFCA in the combination with SHS may cause mild skin irritation with long term usage. Additionally, the topical application of NFCA in combination with SHS resulted in increased skin immune cells from 1793.7±246.1 (0.132 mm^2) to 3380.7±672.9 (0.132 mm^2) for 7 days, indicating a certain degree of skin immune cells infiltration (Figure 6b and c).

Conclusion

In this study, we successfully prepared a novel nanoparticulate formulation of *Cutibacterium acnes* as the main active ingredient and combined it with SHS for transdermal delivery, providing a new and feasible treatment for atopic dermatitis. By comparing particle size, PDI, Zeta potential and protein content, we confirmed the formula composition and preparation scheme of NFCA. In order to further promote the skin penetration of NFCA, we used SHS combined with NFCA for transdermal administration, using FD10K (representing hydrophilic drugs) and DiD (representing lipophilic drugs) as model drugs, which proved that the combination of SHS and NFCA has excellent skin penetration. The penetration effect significantly increases drug absorption in deep skin. At the same time, we also verified through cell experiments that NFCA has cytotoxicity and necessary specific antigenicity. Therefore, we set up different drug dose groups in in vivo animal experiments to verify the effectiveness of SHS combined with NFCA in treating atopic dermatitis at appropriate doses. We

https://doi.org/10.2147/IJN.S509798

confirmed that the combined delivery system was slightly irritating to normal skin. However, its potential application for systemic effects and the immunogenic effect of NFCA will be further investigated in future studies.

Data Sharing Statement

The authors confirm that the data supporting the findings of this study are available within the article.

Acknowledgments

We sincerely thank Shaopeng Yu and Fu Chen for their valuable contribution to the acquisition and maintenance of mice used in this research. Their expertise and dedicated management of the animal center played a pivotal role in facilitating the successful execution of our research endeavors.

Funding

This work was supported by a grant (FJHJF−L-2023-32) from the Fujian Ocean and Fisheries Department, a grant (21CZP002HJ05) from Xiamen Marine and Fisheries Development Fund, a grant (2023XAKJ0101003) from the Scientific Research Foundation of State Key Laboratory of Vaccines for Infectious Diseases, Xiang An Biomedicine Laboratory, a grant (Z20220742) from Pingtan Research Institute of Xiamen University and Shenzhen Science and Technology Program (JCYJ20210324121800003).

Disclosure

Prof. Dr. Ming Chen reports a patent CN202410345869.3 pending and two patents ZL 201610267764.6 and US 10,555,896 B2 issued. The authors report no other conflicts of interest in this work.

References

1. Eichenfield LF, Hanifin JM, Beck LA, et al. Atopic dermatitis and asthma: parallels in the evolution of treatment. *Pediatrics*. 2003;111(3):608–616. doi:10.1542/peds.111.3.608
2. Laughter MR, Maymone MBC, Mashayekhi S, et al. The global burden of atopic dermatitis: lessons from the Global Burden of Disease Study 1990–2017. *Br J Dermatol*. 2020;184(2):304–309. doi:10.1111/bjd.19580
3. Wollenberg A, Schnopp C. Evolution of conventional therapy in atopic dermatitis. *Immunol Allergy Clin North Am*. 2010;30(3):351–368. doi:10.1016/j.iac.2010.06.005
4. Yosipovitch G, Berger T, Fassett MS. Neuroimmune interactions in chronic itch of atopic dermatitis. *J Eur Acad Dermatol Venereol*. 2019;34 (2):239–250. doi:10.1111/jdv.15973
5. Frazier W, Bhardwaj N. Atopic Dermatitis: diagnosis and Treatment. *Am Fam Physician*. 2020;101(10):590–598.
6. Furue K, Ito T, Tsuji G, et al. The IL −13– OVOL 1– FLG axis in atopic dermatitis. *Immunology*. 2019;158(4):281–286. doi:10.1111/imm.13120
7. Towell AM, Feuillie C, Vitry P, et al. Staphylococcus aureus binds to the N-terminal region of corneodesmosin to adhere to the stratum corneum in atopic dermatitis. *Proc Natl Acad Sci*. 2020;118:e2014444118.
8. Fujii M. Current Understanding of Pathophysiological Mechanisms of Atopic Dermatitis: interactions among Skin Barrier Dysfunction, Immune Abnormalities and Pruritus. *Biol Pharm Bull*. 2020;43(1):12–19. doi:10.1248/bpb.b19-00088
9. Kim J, Han Y, Ahn JH, Kim SW, Lee SI, Ahn K. Airborne formaldehyde causes skin barrier dysfunction in atopic dermatitis. *Br J Dermatol*. 2016;175(2):357–363. doi:10.1111/bjd.14357
10. Sroka-Tomaszewska J, Trzeciak M. Molecular Mechanisms of Atopic Dermatitis Pathogenesis. *Int J mol Sci*. 2021;22(8):4130. doi:10.3390/ijms22084130
11. Kim KH. Overview of atopic dermatitis. *Asia Pacific Allergy*. 2013;3(2):79–87. doi:10.5415/apallergy.2013.3.2.79
12. Boyanova L. Cutibacterium Acnes (Formerly Propionibacterium Acnes): friend or Foe? *Future Microbiol*. 2023;18(4):235–244. doi:10.2217/fmb-2022-0191
13. Dreno B, Khammari A, Roques C, Veraldi S, Khammari A, Roques C. Cutibacterium acnes (Propionibacterium acnes) and acne vulgaris: a brief look at the latest updates. *J Eur Acad Dermatol Venereol*. 2018;32(Suppl 2):5–14. doi:10.1111/jdv.15043
14. Nakamura K, O'Neill AM, Williams MR, et al. Short chain fatty acids produced by Cutibacterium acnes inhibit biofilm formation by Staphylococcus epidermidis. *Sci Rep*. 2020;10(1):21237. doi:10.1038/s41598-020-77790-9
15. Francuzik W, Franke K, Schumann RR, Heine G, Worm M. Propionibacterium acnes Abundance Correlates Inversely with Staphylococcus aureus: data from Atopic Dermatitis Skin Microbiome. *Acta Derm Venereol*. 2018;98(5):490–495. doi:10.2340/00015555-2896
16. Rozas M, Fabrega MJ, Brillet F, Brillet F, Brillet F, Brillet F. From Dysbiosis to Healthy Skin: major Contributions of Cutibacterium acnes to Skin Homeostasis. *Microorganisms*. 2021;9(3):628. doi:10.3390/microorganisms9030628
17. Dreno B. What is new in the pathophysiology of acne, an overview. *J Eur Acad Dermatol Venereol*. 2017;31(5):8–12. doi:10.1111/jdv.14374
18. Zhu T, Wu W, Yang S, He L, Sun D, He L. Polyphyllin I Inhibits Propionibacterium acnes-Induced Inflammation In Vitro. *Inflammation*. 2018;42 (1):35–44. doi:10.1007/s10753-018-0870-z
19. Kistowska M, Meier B, Proust T, et al. Propionibacterium acnes Promotes Th17 and Th17/Th1 Responses in Acne Patients. *J Invest Dermatol*. 2015;135(1):110–118. doi:10.1038/jid.2014.290

20. Kitagawa H, Yamanaka K, Kakeda M, et al. Propionibacterium acnes vaccination induces regulatory T cells and Th1 immune responses and improves mouse atopic dermatitis. *Experimental Dermatol*. 2011;20(2):157–158. doi:10.1111/j.1600-0625.2010.01180.x
21. Ale I, Lachapelle JM, Maibach HI. Skin tolerability associated with transdermal drug delivery systems: an overview. *Adv Ther*. 2009;26 (10):920–935. doi:10.1007/s12325-009-0075-9
22. Sabbagh F, Kim BS. Recent advances in polymeric transdermal drug delivery systems. *J Control Release*. 2022;341:132–146. doi:10.1016/j.jconrel.2021.11.025
23. Prausnitz MR, Langer R. Transdermal drug delivery. *Nat Biotechnol*. 2008;26(11):1261–1268. doi:10.1038/nbt.1504
24. Kovacik A, Kopecna M, Vavrova K. Permeation enhancers in transdermal drug delivery: benefits and limitations. *Expert Opin Drug Deliv*. 2020;17 (2):145–155. doi:10.1080/17425247.2020.1713087
25. Andrade JFM, Cunha-Filho M, Gelfuso GM, Gratieri T. Iontophoresis for the cutaneous delivery of nanoentraped drugs. *Expert Opin Drug Deliv*. 2023;20(6):785–798. doi:10.1080/17425247.2023.2209719
26. Park D, Lee S, Lee S, Lee S. Sonophoresis in transdermal drug deliverys. *Ultrasonics*. 2014;54:56–65. doi:10.1016/j.ultras.2013.07.007
27. Dermol-Cerne J, Pirc E, Miklavcic D. Mechanistic view of skin electroporation - models and dosimetry for successful applications: an expert review. *Expert Opin Drug Deliv*. 2020;17(5):689–704. doi:10.1080/17425247.2020.1745772
28. Lima AL, Gratieri T, Cunha-Filho M, Gelfuso GM. Polymeric nanocapsules: a review on design and production methods for pharmaceutical purpose. *Methods*. 2022;199:54–66. doi:10.1016/j.ymeth.2021.07.009
29. Faraji Rad Z, Prewett PD, Davies GJ. An overview of microneedle applications, materials, and fabrication methods. *Beilstein J Nanotechnol*. 2021;12:1034–1046. doi:10.3762/bjnano.12.77
30. Zhang S, Ou, H, Liu C, Wang D, Chen M. Skin Delivery of Hydrophilic Biomacromolecules Using Marine Sponge Spicules. *Mol Pharm*. 2017;14 (9):3188–3200. doi:10.1021/acs.molpharmaceut.7b00468
31. Zhang C, Zhang J, Chen M, et al. Skin delivery of hyaluronic acid by the combined use of sponge spicules and flexible liposomes. *Biomater Sci*. 2019;7(4):1299–1310. doi:10.1039/C8BM01555D
32. Yu L, Li FR, Li X, et al. Topical Application of Exosomes Derived from Human Umbilical Cord Mesenchymal Stem Cells in Combination with Sponge Spicules for Treatment of Photoaging. *Int J Nanomed*. 2020;15:2859–2872. doi:10.2147/IJN.S249751
33. Zhang C, Duan J, Huang Y, Chen M. Enhanced Skin Delivery of Therapeutic Peptides Using Spicule-Based Topical Delivery Systems. *Pharmaceutics*. 2021;13(12):2119. doi:10.3390/pharmaceutics13122119
34. Liang X, Zhang J, Ou H, Chen J, Mitragotri S, Chen M. Skin Delivery of siRNA Using Sponge Spicules in Combination with Cationic Flexible Liposomes. *mol Ther Nucleic Acids*. 2020;20:639–648. doi:10.1016/j.omtn.2020.04.003
35. Draize JH, Woodard G, Calvery HO. METHODS FOR THE STUDY OF IRRITATION AND TOXICITY OF SUBSTANCES APPLIED TOPICALLY TO THE SKIN AND MUCOUS MEMBRANES. *J Pharmacol Exp Ther*. 1944;82(3):377–390. doi:10.1016/S0022-3565(25)08751-8
36. Herrera-Rodríguez SE, López-Rivera RJ, García-Márquez E, Estarrón-Espinosa M, Espinosa-Andrews H. Mexican oregano (Lippia graveolens) essential oil-in-water emulsions: impact of emulsifier type on the antifungal activity of Candida albicans. *Food Sci Biotechnol*. 2018;28 (2):441–448. doi:10.1007/s10068-018-0499-6
37. Schuler CF, Billi AC, Maverakis E, Tsoi LC, Gudjonsson JE. Novel insights into atopic dermatitis. *J Allergy Clin Immunol*. 2023;151 (5):1145–1154. doi:10.1016/j.jaci.2022.10.023
38. Murray PJ, Wynn TA. Protective and pathogenic functions of macrophage subsets. *Nat Rev Immunol*. 2011;11(11):723–737. doi:10.1038/nri3073
39. Medzhitov R. Inflammation 2010: new Adventures of an Old Flame. *Cell*. 2010;140(6):771–776. doi:10.1016/j.cell.2010.03.006
40. Medzhitov R. Origin and physiological roles of inflammation. *Nature*. 2008;454(7203):428–435. doi:10.1038/nature07201
41. Biedermann T, Röcken M, Carballido JM. TH1 and TH2 Lymphocyte Development and Regulation of TH Cell–Mediated Immune Responses of the Skin. *J Invest Dermatol Symp Proc*. 2004;9(1):5–14. doi:10.1111/j.1087-0024.2004.00829.x
42. Roubille C, Martel-Pelletier J, Haraoui B, Tardif JC, Pelletier JP. Biologics and the cardiovascular system: a double-edged sword. *Antiinflamm Antiallergy Agents Med Chem*. 2013;12(1):68–82. doi:10.2174/1871523011312010009
43. Bent R, Moll L, Grabbe S, Bros M. Interleukin-1 Beta—A Friend or Foe in Malignancies? *Int J mol Sci*. 2018;19(8):2155. doi:10.3390/ijms19082155
44. Li M, Hener P, Zhang Z, Kato S, Metzger D, Chambon P. Topical vitamin D3 and low-calcemic analogs induce thymic stromal lymphopoietin in mouse keratinocytes and trigger an atopic dermatitis. *Proc Natl Acad Sci U S A*. 2006;103(31):11736–11741. doi:10.1073/pnas.0604575103
45. Pellefigues C. IgE Autoreactivity in Atopic Dermatitis: paving the Road for Autoimmune Diseases? *Antibodies*. 2020;9(3):47. doi:10.3390/antib9030047
46. Kasperkiewicz M, Schmidt E, Ludwig RJ, Zillikens D. Targeting IgE Antibodies by Immunoadsorption in Atopic Dermatitis. *Front Immunol*. 2018;9:254. doi:10.3389/fimmu.2018.00254